Negative magnetoresistance and sign change of the planar Hall effect due to negative off-diagonal effective mass in Weyl semimetals

Akiyoshi Yamada and Yuki Fuseya
Department of Engineering Science, University of Electro-Communications, Chofu, Tokyo 182-8585, Japan

(Received 15 November 2021; revised 24 February 2022; accepted 10 May 2022; published 31 May 2022)

We theoretically investigated the magnetoresistance (MR) and planar Hall effect (PHE) in Weyl semimetals based on the semiclassical Boltzmann theory, focusing on the fine structure of the band dispersion. We identified that the negative longitudinal MR and sign change in the PHE occur because of the negative off-diagonal effective mass with no topological effects or chiral anomaly physics. Our results highlight the important role of the off-diagonal effective mass, which can cause anomalous galvanomagnetic effects. We propose that the PHE produces a dip in the temperature dependence, which enables the experimental detection of the singularity of effective mass, i.e., the Weyl point.

DOI: 10.1103/PhysRevB.105.205207

I. INTRODUCTION

The galvanomagnetic effect has played a crucial role in solid state physics for many years. For example, the Hall effect is used to determine charge-carrier densities, and the transverse magnetoresistance (TMR) is used to calculate mobilities [1–3]. Extremely sensitive magnetic sensors have been fabricated using the planar Hall effect (PHE) [4,5]. The microscopic origin of the galvanomagnetic effect is the Lorentz force, which is solely a classical effect. Hence, one would anticipate that the theoretical investigation of galvanomagnetic effects is straightforward without any difficulty. In reality, however, this is not the case. For example, it is often explained that the longitudinal magnetoresistance (LMR), where the electric current and magnetic field are parallel, cannot be realized because the Lorentz force does not exist under this condition. By contrast, many materials are known to exhibit LMR [6–8]. The same phenomenon also occurs under the PHE. Although the microscopic origin of the phenomena is clearly understood as the Lorentz force, accurately predicting how the macroscopic galvanomagnetic effect is altered in actual materials remains challenging.

Recently, anomalous galvanomagnetic effects, which cannot be interpreted by the conventional theory, have been observed in various materials [9–17] and have attracted renewed interest from the viewpoint of the chiral anomaly [18–23], the Berry curvature [24–26], or other mechanisms [27,28]. In Weyl electron systems, the charge conservation is violated between different chiralities under a magnetic field that is parallel to the electric field; this phenomenon is referred to as chiral anomaly [18]. The consequence of the chiral anomaly is a negative LMR [19,21]. Moreover, a secondary consequence of the chiral anomaly is angular oscillation with a period π in the PHE where the magnetic field is rotated in the plane parallel to the current [22,23]. Several experimental studies have suggested the possibility of detecting chiral anomaly based on the aforementioned negative LMR [9–12] and PHE [11,13–17]. These anomalous behaviors cannot be interpreted on the basis of *simple* semiclassical theory, and thus, they are believed to be evidence of chiral anomaly.

However, another possibility exists. The *simple* semiclassical theory fails to explain the anomalous LMR and PHE because most semiclassical formulas assume a spherical or an ellipsoidal Fermi surface and do not consider the fine structure of the band dispersion of carriers [29–31]. A detailed evaluation of the characteristic band structure may yield a correct solution. The formula derived by Chambers accounts for the arbitrary shape of the Fermi surface in terms of the velocity, i.e., up to the first-order derivative of energy dispersion for $\boldsymbol{k}$ [1,32]. Recently, the semiclassical formula provided by Mackey-Sybert was extended to account for the arbitrary shape of the Fermi surface through the $\boldsymbol{k}$-dependent effective mass, i.e., up to the second-order derivative of energy dispersion [Eq. (2)] [33]. The extended Mackey-Sybert formula can explain the LMR even with a single closed Fermi surface [33], which is experimentally well known but has never been theoretically obtained based on the *simple* semiclassical theory. The key to explain the LMR with a single closed Fermi surface lies in the off-diagonal effective mass, which reflects the detailed geometrical characteristics of the Fermi surface. The $\boldsymbol{k}$-dependent effective mass can yield galvanomagnetic effects that cannot be predicted based on the simple semiclassical theory [33].

Herein, we show that the negative LMR and the sign change in the PHE are realized in Weyl semimetals based on the extended Mackey-Sybert formula, even without topological effects, the Berry curvature, or the chiral anomaly. Among these anomalous galvanomagnetic effects, the off-diagonal effective mass, which is singular in Weyl semimetals, plays a crucial role.

II. THEORY

We employ the standard model of Weyl semimetals, which is expressed using the following Hamiltonian [34,35]:

$$H = A(k_x\sigma_x + k_y\sigma_y) + M\left(k_w^2 - k^2\right)\sigma_z, \tag{1}$$

where $\sigma_{x,y,z}$ are the Pauli matrices, M and k_w are the model parameters, and $k^2 = k_x^2 + k_y^2 + k_z^2$. A represents the strength of the Weyl nature, which couples the electron and hole bands. M denotes the inverse mass of the electron and hole bands. The eigenenergy of this Hamiltonian is $E(\boldsymbol{k}) = \pm\sqrt{M^2(k_w^2 - k^2)^2 + A^2(k_x^2 + k_y^2)}$. Equation (1) is termed the "Weyl semimetal" model because the first term corresponds to two-dimensional Weyl electrons and the second term corresponds to the ordinary semimetals with free electrons and holes, the extrema of which are located at the Γ point ($\boldsymbol{k} = 0$). The energy dispersions for $M = 16$ eV Å^2 and $k_w = 0.01$ Å^{-1} are shown in Fig. 1(a). The bands cross linearly at the Weyl point, $\boldsymbol{k} = (0, 0, \pm k_w)$. The gap opens at $\boldsymbol{k} = (\pm k_w, \pm k_w, 0)$ with increasing A. Although the energy dispersion changes continuously as a function of A, the shape of the Fermi surface changes discontinuously as shown later. The charge neutrality is maintained only when the Fermi energy E_F is located at the Weyl point. In practice, E_F rarely coincides with the Weyl point. Therefore, hereinafter, we assume E_F to be located slightly above the Weyl point, $E_F = 1$ meV, where the electron carriers are slightly larger than the hole carriers. The conclusions are independent of the sign of E_F in our model.

The Fermi surfaces are shown in Fig. 1 for $A = 0.02$, 0.105, 0.11, and 0.24 eV Å. For small A values, a large electron and a small hole spherical Fermi surface appear concentrically. In other words, the system is semimetallic. As A increases, the electron Fermi surface becomes dented around the equator, whereas the hole Fermi surface swells. The electron surface touches the hole surface along the equator at $A_0 = [2M^2k_w^2 - 2\sqrt{M^2(M^2k_w^4 - E_F^2)}]^{1/2}$ ($\simeq$0.106 eV Å in the present case). For $A > A_0$, the Fermi surface is separated into two electron pockets. Specifically, the shape of the Fermi surface changes qualitatively (the Lifshitz transition) from a semimetal ($A < A_0$) to two electron valleys ($A > A_0$). This Lifshitz transition in Weyl semimetals is often overlooked because it is difficult to imagine it only from the perspective energy dispersion. Details about the correspondence between the dispersion and Fermi surface is shown in the Supplemental Material [36].

First, we estimate the MR and PHE using the classical formula of magnetoconductivity [1–3,36]. In the semimetal region ($A < A_0$) [Fig. 1(a)], the isotropic electron and hole carriers exhibit sizable TMR and no LMR. Accordingly, the π-period PHE appears because the PHE is generally $\rho_{\rm PHE} = -\Delta\rho_{\rm diff}\sin\theta\cos\theta$, where $\Delta\rho_{\rm diff} = \rho_\perp - \rho_\parallel$. ($\rho_\perp$ and $\rho_\parallel$ are the resistivity under the magnetic field perpendicular and parallel to the electric current, respectively.) By contrast, in the two-electron-valley region $A > A_0$ [Fig. 1(d)], the Fermi surfaces can be approximated to two parallel ellipsoids, which are equivalent to a double-size single ellipsoid. In such a case, both TMR and LMR (and so PHE) will vanish. Thus, it is naively expected that the amplitude of TMR and PHE would decrease as A increases and that LMR would remain vanishingly small.

Now, we accurately calculate the magnetoconductivity tensor based on the semiclassical Boltzmann theory. The semiclassical formula derived by Mackey and Sybert [31] has been extended to consider the arbitrary shape of the Fermi surface in the following

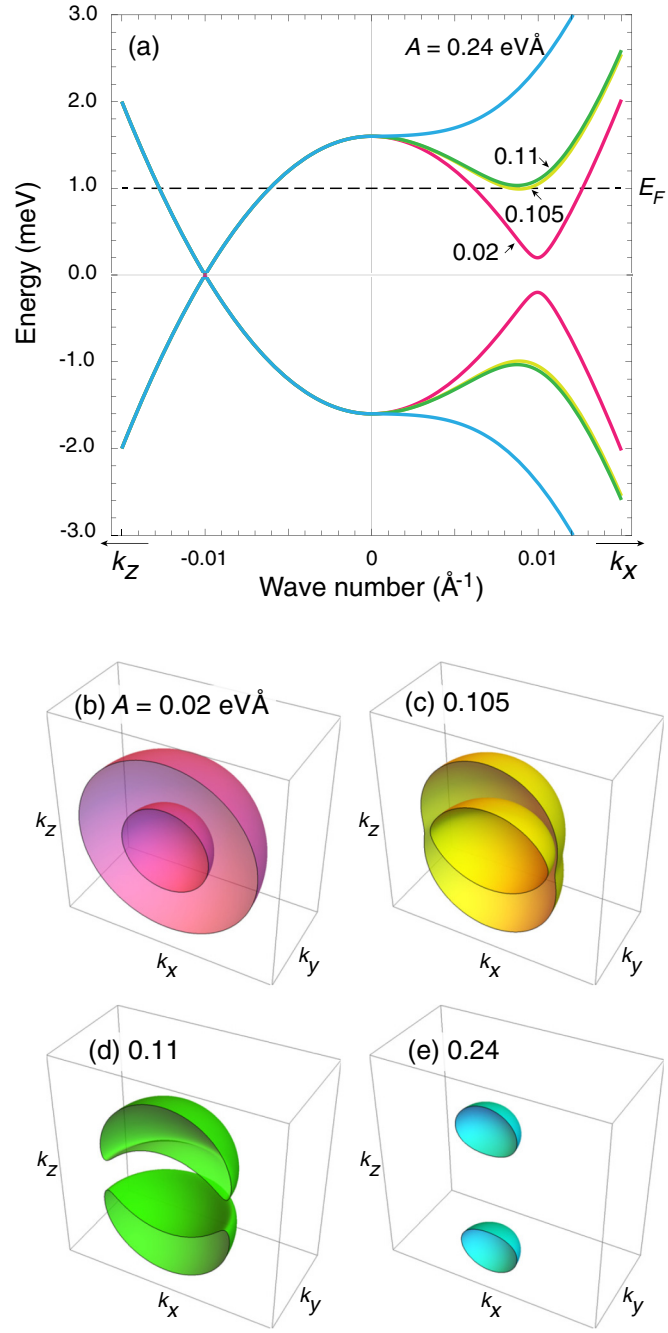

FIG. 1. (a) Band dispersion in the Weyl semimetal model, Eq. (1), for $A = 0.02, 0.105, 0.11, 0.24$ eV Å. (b)–(e) Cross sections of the Fermi surface of a Weyl semimetal for $E_F = 1$ meV: (a) semimetal, (b) semimetal near the Lifshitz transition $A = A_0$, (c) two electron valleys near $A = A_0$, and (d) two electron valleys.

form [33]:

$$\sigma_{\lambda,\mu} = e\langle v_\lambda\{\boldsymbol{v}\cdot[(e\tau)^{-1} - \hat{B}\cdot\hat{\alpha}_{\boldsymbol{k}}]^{-1}\}_\mu\rangle_F, \qquad (2)$$

where e (>0) is the elementary charge, τ is the relaxation time, $\boldsymbol{v}_{\boldsymbol{k}} = \nabla_{\boldsymbol{k}}E/\hbar$ is the velocity, and $\alpha_{\boldsymbol{k}\mu\nu} = \hbar^{-2}\partial^2E/\partial k_\mu\partial k_\nu$ is the inverse of the $\boldsymbol{k}$-dependent effective-mass tensor, which represents the curvature of the equienergy surface. $\hat{B}$ is the magnetic field tensor given as $B_{\lambda\mu} = -\epsilon_{\lambda\mu\nu}B_\nu$ ($\epsilon_{\lambda\mu\nu}$: the Levi-Civita symbol) [31]. $\langle\cdots\rangle_F =$

$\int(\boldsymbol{dk}/4\pi^3)\cdots(-\partial f_0/\partial E)$ corresponds to integration along the Fermi surface at low temperatures, where f_0 is the Fermi distribution function without the magnetic field.

Based on the extended Mackey-Sybert formula, Eq. (2), the coefficient of the magnetic field is generally an effective-mass tensor, i.e., the electron's orbital motion is coupled with the magnetic field through the effective mass. Importantly, this formula does not include any topological effects, such as the Berry curvature and the chiral anomaly. Although the semiclassical equation of motion can include the Berry curvature term [37], in this study, we focus only on the orbital origin of galvanomagnetic effect by considering the detailed structure of the Fermi surface. The unusual behaviors of galvanomagnetic effects, as discussed subsequently, are simply due to the nonuniform effective mass in Weyl semimetals. Moreover, our calculation is restricted at the low magnetic fields where the Landau quantization is not prominent. Oppositely, the chiral anomaly would clearly appear in the quantum limit, where the lowest Landau level dominates the electron transport, in the sense of the Nielsen and Ninomiya theory [18].

III. RESULTS AND DISCUSSION

The results obtained using Eq. (2) are shown in Fig. 2. (In Figs. 2 and 3, we show the results with $\tau = 1.0$ ps.) In the present study, the current orientation was fixed along the x direction, and the magnetic field was rotated in the x-y plane as $\boldsymbol{B} = (B\cos\theta, B\sin\theta, 0)$. We thus obtained the LMR and TMR for $\theta = 0$ and $\pi/2$. In the semimetallic region ($A = 0.02$ eV Å), a sizable TMR is achieved. Its field dependence is $\Delta\rho_\perp \propto B^2$, which is a typical MR property in semimetals. Near the Lifshitz transition ($A = 0.10$ eV Å), $\Delta\rho_\perp$ is almost unchanged, although the saturation field is rather low. Thus far, the properties of $\Delta\rho_\perp$ are consistent with our classical estimation. In the two-valley region, however, $\Delta\rho_\perp$ exhibits a significant negative MR, contradicting the classical estimation. The behavior of LMR is almost the same as that of TMR, i.e., $\Delta\rho_\parallel \propto B^2$ in the semimetallic region and near the Lifshitz transition, whereas $\Delta\rho_\parallel < 0$ in the two-valley region. (Note that $|\Delta\rho_\parallel| < |\Delta\rho_\perp|$.) The observations regarding the LMR contradict the classical theory, which predicts $\Delta\rho_\parallel = 0$ for the entire range of A. The PHE exhibits an angular dependence of $-\sin 2\theta$ in the semimetallic region ($A \lesssim A_0$), whereas the sign of the angular oscillation is inverted in the two-valley region ($A \gtrsim A_0$). The angular dependence for small A can be explained by the concept of multiple carrier conduction [36]. The origin of this sign change can be easily explained by plotting $\Delta\rho_{\rm diff}$, as shown in Fig. 3(a). The reduction in $\rho_\perp$ is larger than $\rho_\parallel$; hence, $\rho_\perp$ becomes smaller than $\rho_\parallel$ near $A = 0.14$ eV Å, resulting in the sign change in $\Delta\rho_{\rm diff}$.

The negative LMR and TMR in the two-valley region is rather surprising. The simple semiclassical theory does not predict a negative MR even if anisotropy or multicarrier effects are considered [3,38,39]. This negative LMR and TMR in the two-valley region can be attributed to the off-diagonal effective mass, which have not been considered in the simple semiclassical theory. The best approach for understanding the significance of the off-diagonal effective mass is to find the Jones-Zener expansion of the extended Mackey-Sybert formula, Eq. (2) [40]. By expanding $[1/e\tau - \hat{B}\cdot\hat{\alpha}_{\boldsymbol{k}}]^{-1}$ in terms of B, the second-order term of LMR for $\boldsymbol{B} = (B, 0, 0)$ can be expressed as

$$\rho_{xx}^{(2)} = \tau\Lambda_x^2\langle v_z v_x(\alpha_{zx}\alpha_{yy} - \alpha_{xy}\alpha_{yz}) + v_x v_y(\alpha_{xy}\alpha_{zz} - \alpha_{yz}\alpha_{zx})\rangle_F B^2, \quad (3)$$

where $\Lambda_\mu = 1/\langle v_\mu^2\rangle_F$. The first term in the parentheses, which includes one off-diagonal and one diagonal effective mass, $\alpha_{\lambda\mu}\alpha_{\nu\nu}$, dominates the second term, which includes two off-diagonal effective masses. This is because the diagonal term is usually larger than the off-diagonal one. Equation (3) shows that negative LMR can appear when the off-diagonal effective mass becomes negative. Such a situation does occur in Weyl semimetals.

The off-diagonal effective mass α_{zx} in the Weyl semimetal model is plotted for $A = 0.02$, 0.105, 0.11, and 0.24 eV Å in Fig. 4. Although α_{zx} is an odd function with respect to k_z and k_x, it appears in Eq. (3) as $v_z v_x \alpha_{zx}$, which is an even

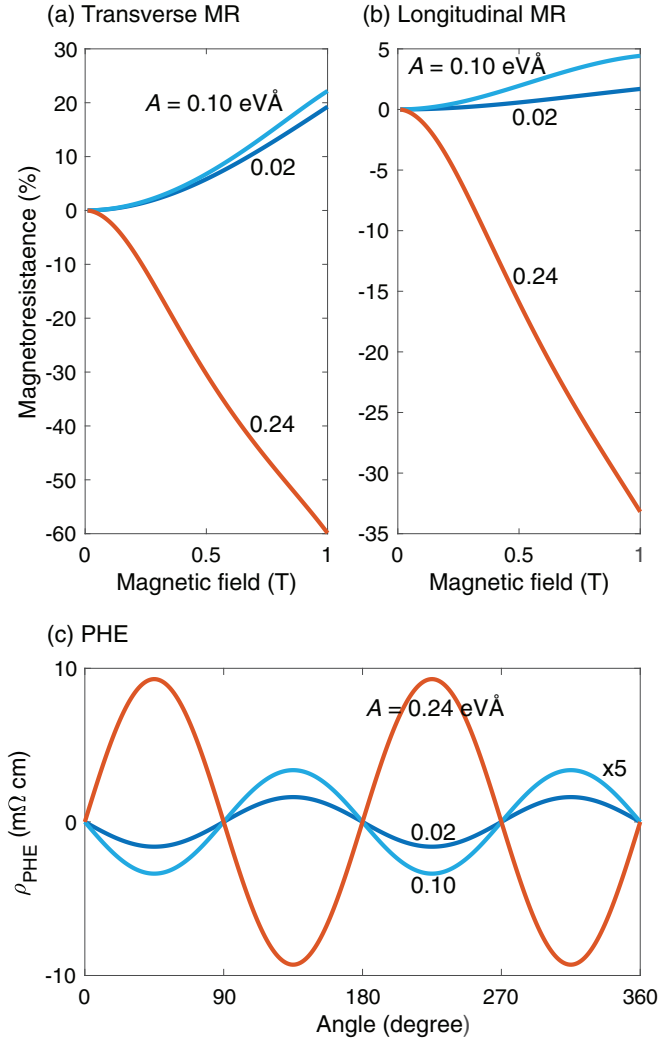

FIG. 2. Magnetic field dependence of (a) transverse and (b) longitudinal MR for $A = 0.02, 0.10, 0.24$ eV Å. (c) Angular dependence of the PHE at $B = 0.5$ T. The PHEs for $A = 0.02, 0.10$ eV Å are amplified fivefold. The temperature is fixed at $T = 0.2$ K for (a) and (b).

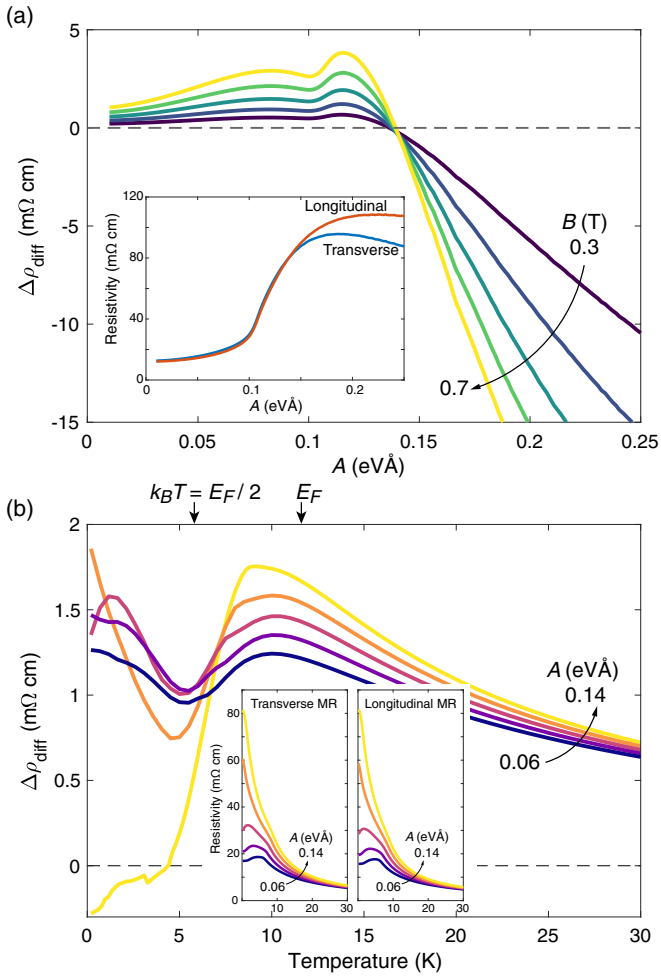

FIG. 3. (a) Difference between TMR and LMR, $\Delta\rho_{\rm diff} = \rho_\perp - \rho_\parallel$, as a function of A at $T = 0.2\,\mathrm{K}$ for $B = 0.3$-$0.7\,\mathrm{T}$. The inset shows the A dependence of $\rho_{\perp,\parallel}$ at $0.5\,\mathrm{T}$. (b) Temperature dependence of $\Delta\rho_{\rm diff}$ at $B = 0.5\,\mathrm{T}$ for $A = 0.06$-$0.14\,\mathrm{eV\,\AA}$. The inset shows the T dependence of $\rho_{\perp,\parallel}$.

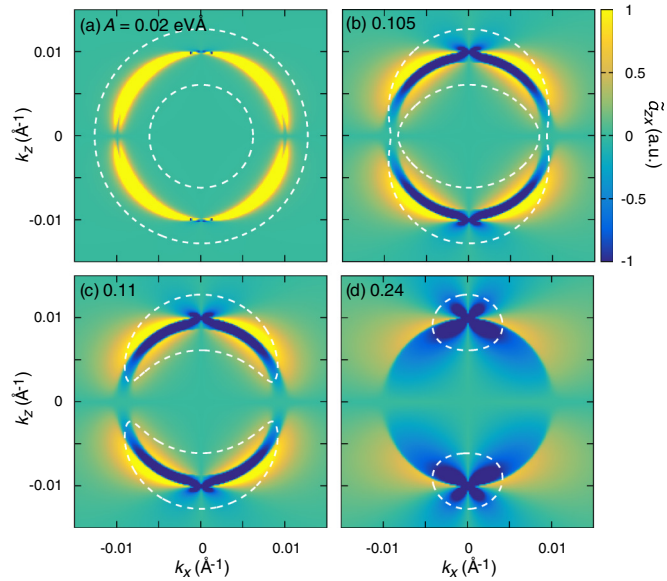

FIG. 4. Off-diagonal effective mass $\tilde{\alpha}_{zx}(k_x, 0, k_z)$ for $A = 0.02, 0.105, 0.11, 0.24$ eV Å. The blue regions correspond to $\tilde{\alpha}_{zx} < 0$. The dashed white lines indicate the Fermi surface. The Weyl points are located at $(k_x, k_z) = (0, \pm 0.01\ \mathrm{Å}^{-1})$.

function. Thus, in Fig. 4, we plot $\tilde{\alpha}_{zx} = \alpha_{zx} v_z v_x / |v_z||v_x|$, which reveals the unusual sign change of the off-diagonal effective mass. The dashed lines indicate the corresponding Fermi surfaces. The blue region corresponds to negative $\tilde{\alpha}_{zx}$. For the semimetallic region (a), the negative-$\tilde{\alpha}_{zx}$ portion is narrow, and the $\tilde{\alpha}_{zx}$ on the Fermi surface is positive for the entire region. The negative-$\tilde{\alpha}_{zx}$ region grows as A increases. Around the Lifshitz transition (b),(c), a part of the Fermi surface has the negative $\tilde{\alpha}_{zx}$, but the positive region remains dominant. In the two-valley region (d), almost the entire Fermi surface has negative $\tilde{\alpha}_{zx}$, which is the dominant contributor to the MR. These results explain the negative LMR in the two-valley region.

In the case of the TMR, $\boldsymbol{B} = (0, B, 0)$, the second-order term is

$$\rho_{xx}^{(2)} = \left[\tau \Lambda_x^2 \left\langle v_x^2 \left(\alpha_{xx}\alpha_{zz} - \alpha_{zx}^2\right)\right\rangle_F - \tau \Lambda_x^2 \Lambda_z \left\langle v_x v_z \alpha_{zx} - v_x^2 \alpha_{zz} \right\rangle_F^2\right] B^2, \quad (4)$$

where the first term originates from the diagonal conductivity, σ_{xx}, and the second one originates from the off-diagonal Hall conductivity, σ_{zx}. The large negative α_{zx} increases σ_{zx} and reduces σ_{xx}. When σ_{zx} dominates σ_{xx}, the negative TMR emerges. Such a condition can actually be satisfied in the case of Weyl semimetals, as shown in Fig. 4.

Some previous studies suggest that negative LMR is evidence of the chiral anomaly [9–12]. In contrast, the present calculation shows that the negative off-diagonal effective mass can cause a negative LMR, which is inherent in Weyl semimetals. In the present model, where the effective mass is isotropic in the x-y plane, the negative LMR is accompanied by the negative TMR. This is due to the oversimplification of the model of Weyl semimetals. $\Delta\rho_\perp > 0$ and $\Delta\rho_\parallel < 0$ can be obtained by considering the detailed band structure of Weyl semimetals. For example, $\Delta\rho_\perp > 0$ and $\Delta\rho_\parallel < 0$ were obtained for the model of $SrTiO_3$ using the extended Mackey-Sybert formula [33].

Finally, we discuss the temperature T dependence of the MR. The T dependence of $\Delta\rho_{\rm diff}$ is depicted in Fig. 3(b). To observe the effects of the Weyl dispersion as transparently as possible, we assumed τ to be constant for T (note that the anomalous T dependence shown below remains even if we consider the T dependence of τ, which should be a monotonic function of T). $\Delta\rho_{\rm diff}$ is generally expected to be a monotonically decreasing function. However, as shown in Fig. 3(b), $\Delta\rho_{\rm diff}$ exhibits a dip near $T = 5\,\mathrm{K}$. The origin of this dip also lies in the negative off-diagonal effective mass. As shown in Fig. 4, the off-diagonal effective mass is singular and changes its sign around the Weyl points. Therefore, the region around the Weyl point hinders the MR when the tail of the Fermi distribution function reaches the Weyl point with $k_BT \sim E_F/2$; this produces the aforementioned dip. Because the Fermi energy is measured from the Weyl point, this thermal energy corresponds to $|E_F - E_W|/2$, where E_W is the energy of the Weyl point. As A increases, the dip becomes

deeper because the impact of the negative off-diagonal effective mass is amplified. For a sufficiently large A, the dip becomes sufficiently deep for $\Delta\rho_{\rm diff}$ to be negative, even at the zero-temperature limit. The temperature at which $\Delta\rho_{\rm diff}$ attains its maximum value approximately corresponds to the energy difference between the Weyl point and E_F. The dip can be seen more clearly in $\Delta\rho_{\rm diff}$ than in TMR or LMR, where the anomaly is masked by the background T dependence, as shown in the inset of Fig. 3(b). Based on this distinctive property, the energy scale of the Weyl point can be determined by measuring the T dependence of $\Delta\rho_{\rm diff}$.

IV. CONCLUSIONS

In conclusion, we investigated galvanomagnetic effects on the basis of the Boltzmann theory, focusing on the geometrical characteristics of the Fermi surface. We identified that the negative off-diagonal effective mass, which is inherent in Weyl semimetals, causes the negative MR and a sign change in the PHE. Our results highlight the critical role played by the off-diagonal effective mass in the galvanomagnetic effects. The results of this study will help obtain a more intuitive understanding of the anomalous galvanomagnetic effect. For example, one can expect anomalous behavior in the galvanomagnetic effect including negative MR and PHE by calculating the effective mass, which is easily obtained from the band calculations. Another direct consequence of the negative off-diagonal effective mass is the anomalous dip in the T dependence of $\Delta\rho_{\rm diff}$ or the amplitude of the PHE. By measuring the dip structure, we can evaluate the energy difference between E_F and the singularity in the effective mass, i.e., between E_F and the Weyl point for Weyl semimetals. Because the effective mass can be singular even when the two bands are gapped out, the dip can appear in other systems. For example, in gapped Dirac materials, the dip structure would correspond to the energy difference between E_F and the band edge, where the effective mass is the most singular. Nonmonotonic T dependence (including the dip and sign change) has been observed in actual materials [13–15,17]. This dependence can originate from the negative off-diagonal effective mass.

Distinguishing the effective-mass origin from others is still a challenge. An immediate identification cannot be obtained from a qualitative discussion so far. However, our theory can extract the MR from the shape of Fermi surface without ambiguity. It would be ideal to combine MR calculations based on the effective mass and first-principle calculations in real materials. When the observation in Dirac and Weyl materials cannot be explained quantitatively by the effective mass, it can be explained based on nontrivial physics including chiral anomaly or Berry curvature.

Our theory is not restricted to the ideal Weyl semimetals. The results at low temperatures remain the same even when the Weyl point is gapped and chirality is not conservative [28]. Moreover, the arguments in terms of the effective mass are applicable to various materials whose energy dispersion is determined.

ACKNOWLEDGMENTS

We thank B. Fauqué and Z. Zhu for helpful comments. This work is supported by JSPS KAKENHI (Grant No. 19H01850).

[1] C. Kittel, *Quantum Theory of Solids* (Wiley, New York, 1963).
[2] J. M. Ziman, *Principles of the Theory of Solids*, 2nd ed. (Cambridge University Press, Cambridge, UK, 1972).
[3] A. Beer, *Galvanomagnetic Effects in Semiconductors*, Solid State Physics Series (Academic, New York, 1963).
[4] A. Schuhl, F. N. Van Dau, and J. R. Childress, Low-field magnetic sensors based on the planar Hall effect, Appl. Phys. Lett. **66**, 2751 (1995).
[5] H. X. Tang, R. K. Kawakami, D. D. Awschalom, and M. L. Roukes, Giant Planar Hall Effect in Epitaxial (Ga,Mn)As Devices, Phys. Rev. Lett. **90**, 107201 (2003).
[6] R. S. Allgaier and W. W. Scanlon, Mobility of electrons and holes in PbS, PbSe, and PbTe between room temperature and 4.2 K, Phys. Rev. **111**, 1029 (1958).
[7] B. Lüthi, Longitudinal Magnetoresistance of Metals in High Fields, Phys. Rev. Lett. **2**, 503 (1959).
[8] J. O. Strom-Olsen, Longitudinal magnetoresistance in silver and copper between 4.2 and 35 °K, Proc. R. Soc. A **302**, 83 (1967).
[9] X. Huang, L. Zhao, Y. Long, P. Wang, D. Chen, Z. Yang, H. Liang, M. Xue, H. Weng, Z. Fang, X. Dai, and G. Chen, Observation of the Chiral-Anomaly-Induced Negative Magnetoresistance in 3D Weyl Semimetal TaAs, Phys. Rev. X **5**, 031023 (2015).
[10] Q. Li, D. E. Kharzeev, C. Zhang, Y. Huang, I. Pletikosić, A. V. Fedorov, R. D. Zhong, J. A. Schneeloch, G. D. Gu, and T. Valla, Chiral magnetic effect in $ZrTe_5$, Nat. Phys. **12**, 550 (2016).
[11] S. Liang, J. Lin, S. Kushwaha, J. Xing, N. Ni, R. J. Cava, and N. P. Ong, Experimental Tests of the Chiral Anomaly Magnetoresistance in the Dirac-Weyl Semimetals Na_3Bi and GdPtBi, Phys. Rev. X **8**, 031002 (2018).
[12] A. Vashist, R. K. Gopal, and Y. Singh, Anomalous negative longitudinal magnetoresistance and violation of Ohm's law deep in the topological insulating regime in Bi_{1-x} Sb_x, Sci. Rep. **11**, 8756 (2021).
[13] N. Kumar, S. N. Guin, C. Felser, and C. Shekhar, Planar Hall effect in the Weyl semimetal GdPtBi, Phys. Rev. B **98**, 041103(R) (2018).
[14] M. Wu, G. Zheng, W. Chu, Y. Liu, W. Gao, H. Zhang, J. Lu, Y. Han, J. Zhou, W. Ning, and M. Tian, Probing the chiral anomaly by planar Hall effect in Dirac semimetal Cd_3As_2 nanoplates, Phys. Rev. B **98**, 161110(R) (2018).
[15] P. Li, C. H. Zhang, J. W. Zhang, Y. Wen, and X. X. Zhang, Giant planar Hall effect in the Dirac semimetal $ZrTe_{5-\delta}$, Phys. Rev. B **98**, 121108(R) (2018).
[16] P. Li, C. Zhang, Y. Wen, L. Cheng, G. Nichols, D. G. Cory, G.-X. Miao, and X.-X. Zhang, Anisotropic planar Hall effect

in the type-II topological Weyl semimetal WTe_2, Phys. Rev. B **100**, 205128 (2019).
[17] S.-Y. Yang, K. Chang, and S. S. P. Parkin, Large planar Hall effect in bismuth thin films, Phys. Rev. Research **2**, 022029(R) (2020).
[18] H. Nielsen and M. Ninomiya, The Adler-Bell-Jackiw anomaly and Weyl fermions in a crystal, Phys. Lett. B **130**, 389 (1983).
[19] D. T. Son and B. Z. Spivak, Chiral anomaly and classical negative magnetoresistance of Weyl metals, Phys. Rev. B **88**, 104412 (2013).
[20] A. A. Burkov, Chiral Anomaly and Diffusive Magnetotransport in Weyl Metals, Phys. Rev. Lett. **113**, 247203 (2014).
[21] A. A. Burkov, Negative longitudinal magnetoresistance in Dirac and Weyl metals, Phys. Rev. B **91**, 245157 (2015).
[22] S. Nandy, G. Sharma, A. Taraphder, and S. Tewari, Chiral Anomaly as the Origin of the Planar Hall Effect in Weyl Semimetals, Phys. Rev. Lett. **119**, 176804 (2017).
[23] A. A. Burkov, Giant planar Hall effect in topological metals, Phys. Rev. B **96**, 041110(R) (2017).
[24] X. Dai, Z. Z. Du, and H.-Z. Lu, Negative Magnetoresistance without Chiral Anomaly in Topological Insulators, Phys. Rev. Lett. **119**, 166601 (2017).
[25] D. Ma, H. Jiang, H. Liu, and X. C. Xie, Planar Hall effect in tilted Weyl semimetals, Phys. Rev. B **99**, 115121 (2019).
[26] Y.-H. Lei, Y.-L. Zhou, H.-J. Duan, M.-X. Deng, Z.-E. Lu, and R.-Q. Wang, Nontopological chiral chemical potential due to the Zeeman field in magnetic Weyl semimetals, Phys. Rev. B **104**, L121117 (2021).
[27] S. Hikami, A. I. Larkin, and Y. Nagaoka, Spin-orbit interaction and magnetoresistance in the two dimensional random system, Prog. Theor. Phys. **63**, 707 (1980).
[28] A. V. Andreev and B. Z. Spivak, Longitudinal Negative Magnetoresistance and Magnetotransport Phenomena in Conventional and Topological Conductors, Phys. Rev. Lett. **120**, 026601 (2018).
[29] H. Jones and C. Zener, The theory of the change in resistance in a magnetic field, Proc. R. Soc. A **145**, 268 (1934).
[30] F. Seitz, Note on the theory of resistance of a cubic ssemiconductor in a magnetic field, Phys. Rev. **79**, 372 (1950).
[31] H. J. MacKey and J. R. Sybert, Magnetoconductivity of a fermi ellipsoid with anisotropic relaxation time, Phys. Rev. **180**, 678 (1969).
[32] R. G. Chambers, Magneto-resistance effects in the group I metals at high fields, Proc. R. Soc. A **238**, 344 (1957).
[33] Y. Awashima and Y. Fuseya, Longitudinal and transverse magnetoresistance of $SrTiO_3$ with a single closed Fermi surface, J. Phys.: Condens. Matter **31**, 29LT01 (2019).
[34] H.-Z. Lu, S.-B. Zhang, and S.-Q. Shen, High-field magnetoconductivity of topological semimetals with short-range potential, Phys. Rev. B **92**, 045203 (2015).
[35] C. M. Wang, H.-Z. Lu, and S.-Q. Shen, Anomalous Phase Shift of Quantum Oscillations in 3D Topological Semimetals, Phys. Rev. Lett. **117**, 077201 (2016).
[36] See Supplemental Material at http://link.aps.org/supplemental/10.1103/PhysRevB.105.205207 for more information on the shape of the Fermi surface of Weyl electrons and the PHE with the classical theory in multiple carrier systems.
[37] D. Xiao, M.-C. Chang, and Q. Niu, Berry phase effects on electronic properties, Rev. Mod. Phys. **82**, 1959 (2010).
[38] Z. Zhu, B. Fauqué, K. Behnia, and Y. Fuseya, Magnetoresistance and valley degree of freedom in bulk bismuth, J. Phys.: Condens. Matter **30**, 313001 (2018).
[39] Y. Mitani and Y. Fuseya, Large longitudinal magnetoresistance of multivalley systems, J. Phys.: Condens. Matter **32**, 345802 (2020).
[40] T. D. Fuchser, H. J. Mackey, and J. R. Sybert, Anisotropic relaxation times and magnetoconductivity for ellipsoidal energy surfaces: Onsager reciprocity restrictions and Jones-Zener expansions, Phys. Rev. B **2**, 3863 (1970).